A MINERALOGICAL STUDY AND CRYSTAL-STRUCTURE DETERMINATION OF NONMETAMICT EKANITE, ThCa₂Si₈O₂₀

J.T. SZYMAŃSKI AND D.R. OWENS

*Mineral Sciences Laboratories, CANMET, Department of Energy,
Mines and Resources, 555 Booth Street, Ottawa, Ontario K1A 0G1*

A.C. ROBERTS AND H.G. ANSELL

Geological Survey of Canada, 601 Booth Street, Ottawa, Ontario K1A 0E8

GEORGE Y. CHAO

Department of Geology, Carleton University, Ottawa, Ontario K1S 5B6

ABSTRACT

Nonmetamict ekanite, ideally $ThCa_2Si_8O_{20}$, of chemical composition very similar to the metamict gemstone ekanite originally found in Sri Lanka (Ceylon), has been discovered in the Tombstone Mountains, Yukon Territory. The physical and optical properties are described and the X-ray powder pattern is given. Crystalline ekanite is tetragonal, space group $I422$, with a 7.483(3), c 14.893 (6) Å. The structure has been solved and refined to $R = 3.57\%$ from 1319 independent reflections obtained from multiple data sets with $MoK\alpha$ radiation. The structure is closely related to that of the family with general composition $ThK(Na,Ca)$ Si_8O_{20}, which crystallizes in space group $P4/mcc$ and which has been misnamed "ekanite" for many years. True crystalline ekanite has a body-centred unit cell whose dimensions agree closely with that of the material obtained on heating metamict ekanite to above 650°C. The metal co-ordination is remarkably similar in the two types of structures; Th is 8–co-ordinated in a square antiprism of oxygen atoms at 2.405(5) A, and Ca has four nearest oxygen neighbors [2.342(5) A] in a very distorted tetrahedron and four second-nearest neighbors [2.688(5) A] near the midpoints of the faces of the tetrahedron. Sheets of metals at $z = 0$, ½ are separated by a puckered silicate layer that extends infinitely in x, y. The structure is characterized by zeolite-like channels through the silicate layers, where non-structural water can become entrapped.

Keywords: nonmetamict ekanite, $ThCa_2Si_8O_{20}$, crystal-structure determination, anomalous dispersion, chemical analysis, powder XRD pattern, properties, Tombstone Mountains, Yukon Territory.

SOMMAIRE

L'ékanite non métamicte, en théorie $ThCa_2Si_8O_{20}$, de composition chimique très semblable à l'ékanite gemme métamicte trouvée pour la première fois à Sri Lanka (Ceylan), a été découverte au mont Tombstone (Yukon). On décrit les propriétés physiques et optiques et l'on en donne le diagramme de poudre aux rayons X. L'ékanite cristalline est tétragonale, et fait partie du groupe spatial $I422$, avec a 7.483(3), c 14.893(6) Å. On en a résolu la structure, affinée jusqu'à $R = 3.57\%$ sur 1319 réflexions indépendantes obtenues à partir de multiples séries de données avec rayonnement de $MoK\alpha$. Sa structure est étroitement associée à celle de la famille de composition générale $ThK(Na,Ca)$ Si_8O_{20}, qui cristallise dans le groupe spatial $P4/mcc$ et qu'on a appelée, à tort, "ékanite" pendant de nombreuses années. La véritable ékanite cristalline possède une maille centrée dont les dimensions sont presque identiques à celles de la matière obtenue lorsqu'on chauffe à plus de 650°C l'ékanite métamicte. Il faut remarquer que la coordinence autour des métaux est la même dans les deux types de structures: le Th, en coordinence 8, se trouve entouré d'atomes d'oxygène distants de 2.405(5) Å et formant un anti-prisme à base carrée; le Ca a quatre premiers voisins très proches [2.342(5) Å] en tétraèdre difforme et quatre seconds voisins [2.688(5) Å] près de points intermédiaires des faces du tétraèdre. Les feuillets de métal à $z = 0$, ½ sont séparés par une couche déformée de silicate. La structure est caractérisée, comme celle des zéolites, par des canaux qui traversent les couches de silicate, où l'eau non structurale peut être piégée.

Mots-clés: ékanite non métamicte, $ThCa_2Si_8O_{20}$, détermination de la structure, dispersion anormale, analyse chimique, diagramme de poudre aux rayons X, propriétés, mont Tombstone (Yukon).

INTRODUCTION

The mineral *ekanite* $(Th,U)(Ca,Fe,Pb)_2Si_8$ O_{20} was first reported (Anderson *et al.* 1961) as a green transparent to translucent metamict

gemstone. It was described in great detail by Gübelin (1961, 1962) in terms of its physical properties, radioactivity, chemical composition, inclusions and gem qualities. The original report of Anderson *et al.* (1961) stated that "At temperatures between 650 and 1000°C, the mineral re-crystallizes to a phase of which X-ray powder and single-crystal diffraction patterns can be indexed on the basis of a body-centred tetragonal cell having dimensions *a* 7.46, *c* 14.96 Å. The density after heating at 1000°C for 24 hr. rises to 3.313 and the mineral becomes opaque putty-coloured".

Since then, the crystal structures of a family of minerals of composition similar to ekanite, but with about half of the calcium ions replaced by a sodium, and with an additional potassium ion, have been reported (Mokeyeva & Golovastikov 1966, Richard & Perrault 1972). The latter report clearly shows the incomplete site-occupancies at all the metal sites, and indicates that the (Na,Ca) and K ions occupy different sites in the structure. The space group of the mineral analyzed in both reports was found to be *P4/mcc*, with *a* 7.58, *c* 14.77 Å (Richard & Perrault 1972) for the material found at St-Hilaire, Québec, and *a* 7.58, *c* 14.82 Å (Mokeyeva & Golovastikov 1966) for the material found in Central Asia. Iraqite (Livingstone *et al.* 1976), which is closely related to the latter two minerals, but which shows extensive rare-earth substitution for thorium and calcium, has also been described. It too has space group *P4/mcc* and similar cell dimensions.

Despite the original report that metamict ekanite recrystallized thermally to a body-centred phase, the name "ekanite" or "ekanite-family" has been retained in all cases of structures found to have the primitive tetragonal lattice, space group *P4/mcc*. An additional name, "kanaekanite", was coined by Povarennykh & Dusmatov (1970) to describe the K-containing and Na-for-Ca-substituted material; this name has been used in the literature (Livingstone *et al.* 1976, Hey & Embrey 1974), though I.M.A. approval never was obtained.

Recently, Embrey & Fuller (1980) have raised questions about the validity of ekanite itself ("Formula and status in doubt"), probably as a result of the existence of the K-containing, Na, Ca-substituted phases to which the name ekanite was applied. Perrault & Richard (1973) were particularly apprehensive about the use of the name "ekanite" to describe the St-Hilaire material, but finally followed the Russian usage of that name for the Central Asian material of composition very similar to theirs (Ginzburg

et al. 1965, Mokeyeva & Golovastikov 1966).

The present material, found in a boulder in the Tombstone Mountains, Yukon Territory, has a totally different structure from any of the *P4/mcc* minerals to which the names "ekanite", "ekanite-family" or "kanaekanite" have been applied. Furthermore, it can be identified directly by its Debye-Scherrer powder pattern with the thermally recrystallized metamict ekanite of Anderson *et al.* (1961; priv. comm. from Miss E.J. Fejer to J.T. Szymański, concerning the powder pattern from Dr. Davis's notebook). Thus, it alone truly deserves to carry the name *crystalline ekanite* as opposed to *metamic ekanite*. Nomenclature changes for the other species are indicated or have been accepted by the Commission on New Minerals and Mineral Names (Perrault & Szymański 1982). As a result of a recent decision by this Commission, the St-Hilaire "ekanite" material has been renamed "steacyite" (Perrault & Szymański 1982), and will be referred to by this name henceforth.

Occurrence

Ekanite was found in a glacial syenitic boulder within the Tombstone Mountains, Yukon Territory, at latitude 64°24'N and longitude 138°36'W. The boulder was located in one of the cirques situated on the north side of the Tombstone Mountains and was locally derived from the north-facing wall. Associated minerals, identified by X-ray powder diffraction and thin section study, are fluorite, garnet, quartz, perthitic microcline, clinopyroxene, apatite, sodic plagioclase, hematite, thorogummite, zircon and titanite.

Physical and Optical Properties

Crystalline ekanite is straw-yellow to dark red in color; the darker and redder the color, the more inclusions the material contains. The streak is white, the lustre is vitreous, the tenacity is brittle, and the Mohs hardness is approximately 4½. The mineral does not fluoresce in either long- or short-wave ultraviolet light.

The largest crystals are about 2–3 mm in length, with the average around 1 mm. Ekanite occurs as discrete grains or clusters of grains that, in some cases, approximate subhedral pyramids. The vast majority of grains examined, however, are anhedral in shape. The forms observed are {101}, {110}, {001} and {100}. An idealized crystal drawing is presented in Figure 1. The fracture is irregular; all grains show some degree of fracturing even on a micro scale. The {101} cleavage is distinct, and

{001} indistinct. Crystals are striated parallel to x.

The measured density by Berman balance on 9.42 mg of hand-picked sample is 3.08(5) g cm^{-3}. The calculated density for $(Th_{0.894}U_{0.047})_{\Sigma 0.94}(Ca_{1.912}Fe_{0.059}Mn_{0.029})_{\Sigma 2.0}Si_8O_{20}$ is 3.36 g cm^{-3}. The discrepancy of 10% between the calculated and measured densities may be ascribed to the cumulative effects of impurities and inclusions: hematite and thorogummite inclusions, entrapped air within the numerous microfractures, and non-structural water within the zeolitic channels (see Discussion).

Optically, the mineral is uniaxial negative, with indices of refraction (determined in Na light) ϵ 1.568(3) and ω 1.580(3). The large uncertainty in the indices of refraction stems from the interference of fine grained, red to reddish brown alteration. All crystals studied on the flat stage showed poor interference figures. Some crystals are slightly biaxial negative, with $2V$ 10–15°; some also show zoning. In thin section, under transmitted light and when free of inclusions, ekanite is colorless to straw-yellow. However, in most specimens the reddish alteration is preponderant and makes ekanite readily identifiable in thin section.

Heating of the mineral in a vacuum for three hours at temperatures in excess of 900°C did not destroy the ekanite structure. The only visible change in the X-ray powder-diffraction pattern was the strengthening in intensity of those diffraction lines belonging to the admixed thorogummite phase.

CHEMICAL COMPOSITION

Initial microprobe studies showed that ekanite reacted strongly under the electron beam (2 μm diameter). To minimize this effect, analyses were performed using a defocused electron beam of 10–20 μm, with a closed aperture except during the 10-second counting period. Even under these conditions, degradation of the surface was clearly visible.

There is a significant variation in color between specimens, from deep red to amber. Microscopic comparison of these colors showed that the deep red grains are saturated with inclusions. The amber grains appear to be pure and monophase. Results of microprobe analyses of the amber grains are more consistent than that of the red grains, but still did not yield a sensible chemical composition.

The microprobe results may be stated as follows: 1. Unheated specimen; cations determined by electron microprobe (at G.S.C., analyst G.J. Pringle, average of four analyses).
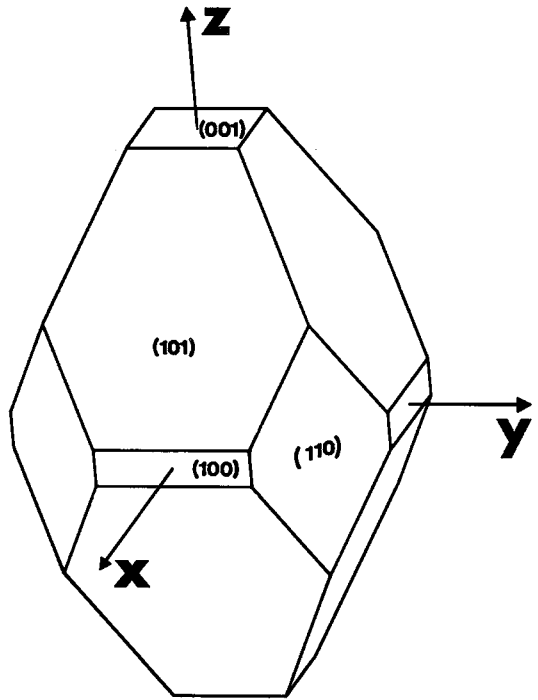

FIG. 1. Idealized crystal drawing of euhedral ekanite.

Experimental conditions: accelerating voltage 20 kV, specimen current ~0.030 μA, counting periods 10 seconds, diameter of electron beam 20 μm (moving beam to minimize beam damage to sample). Standards: wollastonite for Ca and Si, synthetic ThO$_2$ for Th, synthetic UO$_2$ for U, rhodonite for Mn, and kaersutite for Al and Fe. Analysis yielded: SiO$_2$ 45.1, CaO 9.0, ThO$_2$ 36.0, Al$_2$O$_3$ 0.5, UO$_2$ 1.9, FeO 0.3 and Mn 0.2 wt. %; total = 92.9 wt. %. 2. Unheated specimen; cations determined by electron microprobe (at CANMET, analyst D.R. Owens, average for three apparently similar areas). Experimental conditions: accelerating voltage 20 kV, specimen current ~0.025 μA, counting periods 10 seconds, diameter of electron beam ~15 μm. Standards: synthetic ThO$_2$ for Th, synthetic UO$_2$ for U, rhodochrosite for Mn, and kaersutite for Al, Ca and Fe. Analysis yielded: SiO$_2$ 41.7, CaO 8.1, ThO$_2$ 37.1, Al$_2$O$_3$ 1.3, UO$_2$ 0.5, FeO 0.3 and MnO 0.3 wt %; total = 89.3 wt. %. 3. Heated specimen; cations determined by electron microprobe (at CANMET, analyst D.R. Owens, average of four analyses). Experimental conditions: accelerating voltage 20 kV, specimen current ~0.030 μA, counting periods 10 seconds, electron beam diameter ~10 μm. Standards: synthetic ThO$_2$ for Th,

synthetic UO_2 for U, rhodochrosite for Mn, kaersutite for Ca and Fe, and orthoclase for Si. Analysis yielded: SiO_2 47.6, CaO 9.6, ThO_2 37.8, Al_2O_3 0.8, UO_2 1.1, FeO 0.4 and MnO 0.2 wt. %; total = 97.5 wt. %.

Bulk chemical analysis of hand-picked grains, chosen under a binocular microscope, gave 7.8 wt. % H_2O and 3.4 wt. % F.

The observed powder pattern of ekanite shows four lines that could not be indexed on the ekanite cell, but that correspond to the strongest reflections of thorite or thorogummite. These impurities undoubtedly affect the microprobe-derived composition but, provided they are in a finely divided form, they should not affect the single-crystal diffraction pattern. Because of the uncertainty in the chemical composition derived from microprobe analyses, crystal-structure determination was undertaken; it showed that the theoretical composition is $ThCa_2$ Si_8O_{20}. This structure requires SiO_2 56.10, CaO 13.09 and ThO_2 30.81 wt. %. It is not possible to say whether the minor impurities found in the microprobe analyses are present in the ekanite or as part of the thorogummite. Heating experiments on ekanite grains showed some 9% weight loss on heating to 900°C. By analogy with steacyite (Richard & Perrault 1972), the water content may be partly zeolitic as well as contained in the thorogummite.

In summary, the microprobe analyses and the bulk chemical analyses do not reflect the composition of ekanite for several reasons: 1. the presence of zeolitic water in ekanite, which causes the surface of the specimens to bubble and froth during microprobe analysis, 2. the fine grained intergrowth of ekanite with thorogummite, and 3, the numerous fine inclusions in ekanite, in addition to the larger inclusions of hematite.

The single crystal used for data collection in the structure determination was examined extensively with the microprobe after the data collection was complete. It showed numerous inclusions and gave overall results comparable to Analysis No. 2 (above). These values were not used in the crystal-structure determination, except to give the ratios for the composition at the metal sites, *i.e.*, Th:U and Ca:Fe:Mn. The composition of the crystalline ekanite examined was derived crystallographically from these ratios and the refined occupancies at the metal sites.

PRELIMINARY CRYSTALLOGRAPHIC EXAMINATION AND DATA COLLECTION

Examination of a number of crystal frag-

ments with precession photographs showed the crystal structure to be body-centred tetragonal, with a diffraction symmetry approximately $4/mmm$. Deviations from this symmetry in the layers hkl, $l = 1$ to 5, were noted and compared with the layers $l = -1$ to -5. A clear indication that Friedel's Law was *not* obeyed was obtained, and the equivalent general hkl reflections of symmetry $4/mmm$ were divided into two subsets of symmetry 422. This fixed the space group uniquely as $I422$ *from the diffraction symmetry alone*, with Friedel's Law breaking down as a result of the strong anomalous dispersion of thorium (8.87e for MoKα radiation).

No straw-yellow or amber-colored fragments were found suitable for single-crystal data collection, so a red fragment had to be used. The selected crystal was cut into a rough cube and ground to a sphere 0.246 mm in diameter using the Bond method (1951). Examination with a precession camera showed the sphere to be a single crystal, but with a large mosaic spread.

The crystal was mounted on a 4-circle diffractometer in a general orientation. For the determination of cell dimensions, low-angle data had to be used, with a mean Kα wavelength (MoKα = 0.71073 Å), as the large mosaic spread (some 3°) precluded resolving the $α_1$, $α_2$ components within the limits of observable data. The $2θ$, $χ$, $ω$ values of 62 reflections in the range $21° < 2θ < 30°$ were refined by least squares (Busing 1970) to obtain the cell dimensions given in Table 1.

Although normally in space group $I422$, the unique data-segment is 1/16 of the reciprocal sphere; $(hkl, h \geqslant k)$, the presence of the anomalous scatterer made $I_{hkl} \neq I_{khl}$. Consequently, the unique segment was considered as 1/8 of the reciprocal sphere, and three complete octants of data were collected, $(hkl, \bar{k}hl, \bar{h}kl)$, using graphite monochromated MoKα radiation to a limit of $2θ = 80°$. A $θ$–$2θ$ scan was used at a $2θ$ scan rate set to 2° per minute, with the

TABLE 1. CRYSTAL DATA

Source: A boulder in the Tombstone Mountains, Yukon Territory.

Composition:
$(Th_{0.894}U_{0.047})_{\Sigma 0.94}(Ca_{1.912}Fe_{0.059}Mn_{0.029})_{\Sigma 2.00}Si_8O_{20}$

Systematic absences: hkl, $h+k+l = 2n + 1$

Space group: $I422$ (#97).

Cell dimensions: $a = 7.483(3)$, $c = 14.893(6)$Å

Density: measured: 3.08 ± 0.05 g cm^{-3} (microfractured specimen probably containing entrapped air).

calculated: 3.36 g cm^{-3}. (not including water).

Absorption: Spherical crystal, $r = 0.123mm$, $\mu r = 1.13$

scan width adjusted for dispersion (3.0–3.6°). Background counts were made for 30 seconds on ether side of the peak. Three linearly independent standard reflections were recorded every 50 measurements to monitor crystal alignment and instrument stability. Spherical absorption corrections were applied to the data using a fortuitously close estimate of the composition (other than water) and the observed density. The three octants of data were averaged to give 1319 unique reflections, of which 163 were considered "unobserved" on the criterion that $I < 1.65 \times \sigma(I)$.

X-RAY POWDER DIFFRACTION

A fully indexed powder pattern for crystalline ekanite is given in Table 2. This is in excellent agreement with that of the body-centred tetragonal phase obtained by heating Sri Lanka (Singhalese) metamict ekanite above 650°C (priv. comm. 1980 from Miss E.J. Fejer to J.T. Szymański, data from R.J. Davis's notebook).

TABLE 2. X-RAY POWDER DATA FOR EKANITE

#	hkl[1]	d_calc[2]	d_obs[3]	I_o[4]	I_c	#	hkl	d_calc	d_obs	I_o	Ic
1	002	7.446	7.45	58	46	27	420 / 404 / 208	1.673 / 1.672 / 1.667	1.671	15	14
2	101	6.687	6.70	61	73	28	422	1.633	1.632	12	14
3	110	5.291	5.28	9	9	29	307 / 109	1.619 / 1.616	1.618	9	8
4	112	4.313	4.31	14	12	30	415	1.550	1.547	8	5
5	103	4.137	4.14	100	100	31	424 / 228	1.526 / 1.522	1.524	8	9
6	200	3.742	--	--	1	32	406 / 431	1.494 / 1.489	1.489	9	10
7	202	3.343	3.343	96	88	33	219	1.483	--	-	4
8	211	3.265	3.265	65	79	34	318	1.463	1.461	6	3
9	114	3.045	3.044	13	4	35	512 / 336 / 503	1.440 / 1.438 / 1.433	1.436	11	8
10	213 / 105	2.775 / 2.767	2.766	23	22	36	426 / 20.10 / 521	1.387 / 1.384 / 1.384	1.385	14	16
11	220 / 204	2.646 / 2.639	2.642	54	66	37	514	1.365	1.363	5	2
12	222 / 006	2.493 / 2.482	2.494	18	14	38	523 / 505 / 435 / 10.11	1.338 / 1.337 / 1.337 / 1.332	1.335	9	9
13	301	2.460	2.460	22	13	39	408	1.320	1.319	6	4
14	310	2.366	2.361	7	3	40	442	1.302	--	-	2
15	312 / 116	2.255 / 2.247	2.254	14	10	41	329	1.294	1.294	8	4
16	303 / 215	2.229 / 2.225	2.225	22	17	42	532 / 516	1.265 / 1.263	1.261	9	5
17	224	2.157	2.157	22	22	43	525 / 21.11	1.259 / 1.255	--	-	2
18	206 / 321	2.068 / 2.056	2.060	17	23	44	444 / 428 / 602	1.247 / 1.244 / 1.230	1.245	9	7
19	314	1.997	1.996	13	9	45	611 / 437 / 419	1.226 / 1.224 / 1.223	1.224	12	10
20	323 / 305	1.915 / 1.912	1.913	20	24						
21	400 / 008	1.871 / 1.862	1.868	17	17						
22	402 / 226	1.814 / 1.810	1.810	19	16						
23	411 / 217	1.802 / 1.795	1.796	26	32						
24	118	1.756	1.758	11	12						
25	332	1.716	--	--	1						
26	413 / 325	1.705 / 1.703	1.702	19	18						

[1] Although the khl intensity is not equal to the hkl intensity, both are included under the simple index as they are coincident.

[2] Data from POWGEN (Hall & Szymański 1975), powder pattern generating program based on single-crystal intensities.

[3] 114.60 mm Debye-Scherrer camera, CuKα radiation (λ = 1.5418Å), Ni filter.

[4] Intensities calculated from powder diffractometer trace.

Four weak to very weak diffraction lines ascribable to thorogummite were detected on the powder diffraction patterns, but evidence for a crystalline iron-bearing phase was lacking.

During the initial stages of the ekanite investigations, a careful search of the JCPDS Powder Diffraction File indicated similarity between the ekanite and thorosteenstrupine (PDF 16–608) powder patterns. All the lines of the thorosteenstrupine X-ray powder pattern may be successfully indexed by a combination of the ekanite pattern with that of a monazite-structured mineral (perhaps cheralite). Further careful study of type thorosteenstrupine is deemed necessary to validate this mineral as a distinct species.

STRUCTURE DETERMINATION

It was presumed that the structure of ekanite would be related to that of steacyite, $Th_{2-x}(Na,Ca)_{4-y}K_{2-z}Si_{16}O_{40}\cdot nH_2O$ ($x = 0.18$, $y = 0.29$, $z = 0.79$: Richard & Perrault 1972). Both have tetragonal cells of very similar dimensions [a 7.58(1), c 14.77(2) Å for steacyite], though the space groups are different ($I422$ for ekanite, $P4/mcc$ for steacyite).

Accurate microprobe data, which would have yielded a composition and formula for ekanite, were not available at the time of the structure analysis. Consequently, certain assumptions had to be made in order to proceed with the structure determination. It was presumed, for a start, that there were two thorium atoms in the unit cell. For space group $I422$, this fixes Th at the origin.

Two syntheses were calculated: 1. An $(E^2−1)$ vector map. This showed only one large positive peak, corresponding to a Ca position ($\frac{1}{2},0,0$), and a second smaller peak ($\frac{1}{2},\frac{1}{2},0$) for the Ca—Ca vector. Numerous small peaks were found, but not analyzed. 2. A $P_s(r)$ modified Patterson synthesis (Okaya et al. 1955). This synthesis uses as coefficients the difference between F^2_{hkl} and $F^2_{\overline{hkl}}$. If we denote the indices hkl by H,

$$P_s(r) = \frac{1}{v} \Sigma (F^2_H - F^2_{\overline{H}}) \cdot \sin 2\pi H \cdot r$$

The synthesis yields a vector map of the noncentrosymmetric component of the structure, relative to the anomalously scattering atom. In the present case, $F^2_{\overline{hkl}} = F^2_{khl}$, and if we denote ($F^2_H - F^2_{\overline{H}}$) by Δ, then the coefficients of the synthesis are: Δ for hkl, for $h>k$, $-\Delta$ for khl, and 0 for $hk0$, $0kl$, $h0l$, hhl.

The summation was carried out using one

TABLE 3. ATOMIC POSITIONAL AND THERMAL PARAMETERS

Atom	Position	x	y	z	U_{11}	U_{22}	U_{33}	U_{12}	U_{13}	U_{23}
Th	2	0	0	0	103(1)	103(1)	143(2)	0	0	0
Ca	4	½	0	0	158(6)	293(8)	267(8)	0	0	0
Si	16	.3335(2)	.2540(2)	.1479(1)	160(5)	147(5)	220(6)	-5(4)	-7(5)	-15(5)
O(1)	16	.2544(7)	.4521(5)	.1251(3)	262(19)	126(13)	523(28)	25(13)	-13(21)	28(16)
O(2)	8	.2924(8)	½+x	¼	606(37)	606(37)	207(26)	127(44)	69(24)	69(24)
O(3)	16	.2553(6)	.1075(6)	.0818(3)	230(18)	279(20)	291(19)	-25(16)	-70(17)	-81(16)

The anisotropic temperature factors are expressed in the form:

$$T = \exp[-2\pi^2(U_{11}a^{*2}h^2..+.2U_{12}a^*b^*hk..+.)],$$ and the values quoted are x 10^4.

octant of these coefficients in symmetry $I4$. Because in this structure the anomalous scatterer (Th) is at the origin, the synthesis gave a direct determination of the position of the silicate molecule in the cell and its absolute configuration relative to the choice of axes. No other peaks appeared in the resultant map.

The scattering curves used were the neutral atomic species, Th, Ca, Si and O, taken from International Tables (1974). This same source provided values for the anomalous dispersion coefficients for the same atoms. The structure was refined to $R = 6.1\%$ isotropically and $R = 3.7\%$ anisotropically. A difference map at this stage revealed a significant negative peak at the thorium position, indicating incomplete site occupancy.

In view of the unreliable microprobe analyses, no accurate measure of the composition was available. The site-occupancy parameters of the metal sites were allowed to vary. That of Ca increased by about 1%, a feature which can easily be explained by the minor substitution of Fe and Mn for Ca at that site. The site occupancy of Th dropped to 0.94, the residual falling to $R = 3.57\%$. At this stage, a virtually featureless difference map was obtained, with only a few very minor positive areas.

Most of the crystallographic calculations were done using the X-RAY system of programs (Stewart *et al.* 1976). The $P_s(r)$ synthesis was computed using a highly modified version of Zalkin's Fourier program FORDAP.

The rapid decomposition of the crystals under the electron microprobe beam (focused or defocused) and the weight loss of some 9% on heating specimens to 900°C were both indicative of water present in the structure, though the final agreement factor and the lack of any significant peaks in the difference map clearly indicate that this water is non-structural. Infrared measurements on ekanite reveal both free water and bonded hydroxyl (Farrell 1978). However, an attempt was made to locate partially occupied bonded-water sites, based on the very minor peaks in the difference map. All possible sites refined to zero site-occupancy in the least-squares refinement.

The final refined structural parameters are given in Table 3. The observed (10 x F_o) and calculated (10 x F_c) structure factors are given in Table 4, which is available at a nominal charge from the Depository of Unpublished Data, CISTI, National Research Council of Canada, Ottawa, Ontario K1A 0S2.

DESCRIPTION OF THE STRUCTURE

The structure is illustrated in Figure 2. The metals are stacked in layers at $z = 0$, ½ and are separated by a puckered silicate sheet. The coordination of the metals is illustrated in Figure 3. Thorium has the expected square antiprism of oxygens [Th–O(3) = 2.405(5) Å]. The same oxygens that bond to thorium also bond to calcium in a very distorted tetrahedron [Ca–O(3) = 2.342(5) Å]. The centres of the tetrahedral faces are occupied by a set of second-nearest neighbors, these being O(1) at 2.688 (5) Å, and this second tetrahedron is even more distorted.

The silicate network can be described as follows: the four-fold axis at ½,½,z relates four corner-sharing silicate tetrahedra in which the silicon atoms are stacked in the plane $z \simeq ⅛$. These tetrahedra are linked *via* the bridging oxygens O(1), and each Si is connected to two such O(1) atoms. Another oxygen, O(3), is involved in bonding to the neighboring metal atoms (see above). The first square of silicate tetrahedra is linked to four other squares *via* O(2), which is at $z = ¼$. These latter squares are formed around the four-fold axes through
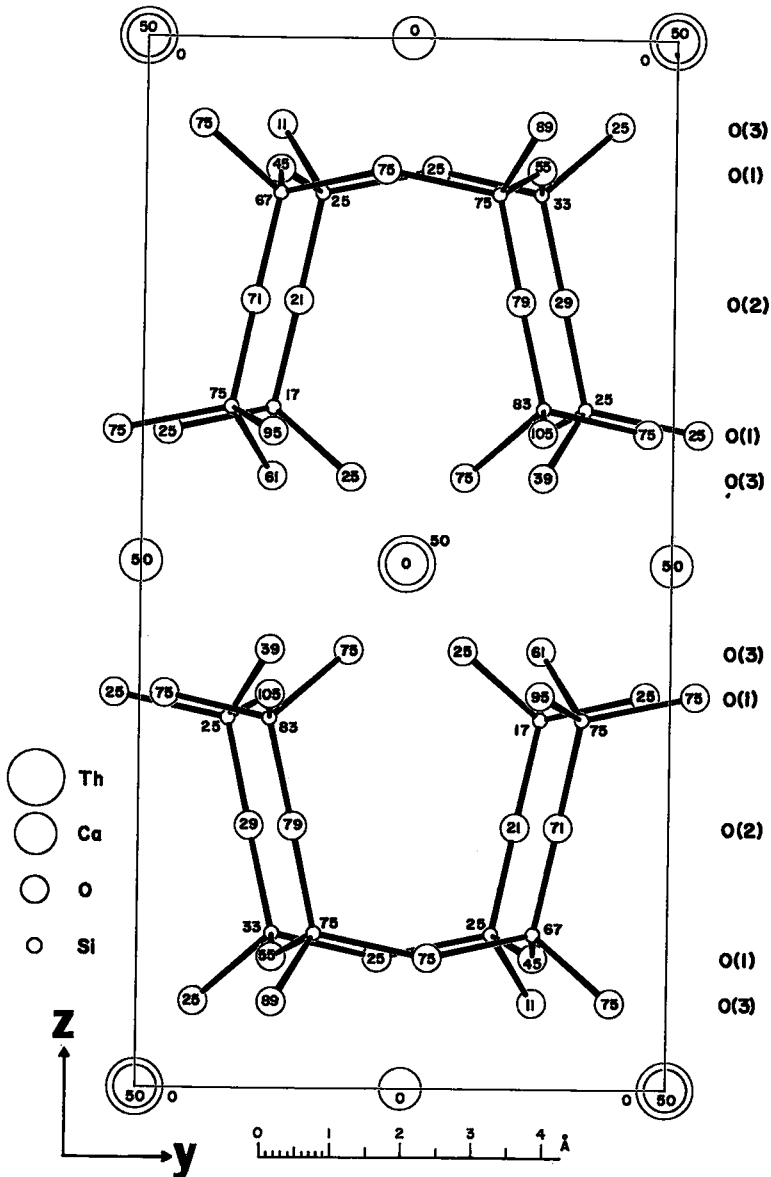
FIG. 2. The structure of ekanite projected on the y–z plane. Fractional coordinates (x 100) in the x direction for each atom are given within or beside the circle representing the atom.

0,0,z, 1.0,z, 0,1,z and 1,1,z. Within the latter four squares, the silicon atoms are stacked in the plane $z \simeq 3/8$. In terms of topology, the structure has a puckered, singly connected infinite sheet of silicate tetrahedra, though within this single sheet, the puckering results in two distinct layers of silicons at $z \simeq 1/8$ and $3/8$. A symmetry-related second sheet, with its two layers of silicon atoms, occurs at $c/2$ away from the first sheet; in this sheet, the silicon atoms are at $z \simeq 5/8$ and $7/8$. Further details of bond lengths and angles in the structure are given in Table 5.

Throughout the structure, there are infinite intersecting channels in the x and y directions, about 4 Å in diameter, at x,0,0.2; x,0,0.8;
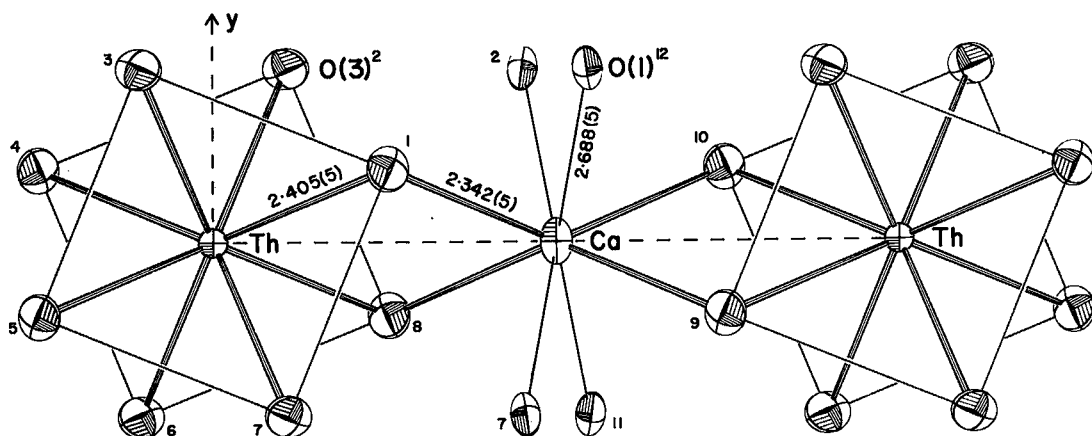
FIG. 3. A view down the z axis showing the co-ordination of the metals along the x axis. The thermal ellipsoids are drawn at 50% probability (Johnson 1965). Legend for the equivalent positions is given in Table 5.

TABLE 5. BOND DISTANCES AND ANGLES WITH STANDARD DEVIATIONS

(a) Thorium coordination, square anti-prism.

Th — O(3) 2.405(5)Å

Non-bonded contacts, (Å).		Angles(°)	
O(3)¹... O(3)³ 2.932(7)		O(3)¹ — Th — O(3)²	74.0(2)
O(3)¹... O(3)² 2.895(6)		O(3)¹ — Th — O(3)⁸	74.8(2)
O(3)¹... O(3)⁸ 2.920(6)		O(3)² — Th — O(3)⁸	75.1(2)
		O(3)¹ — Th — O(3)⁴	140.9(2)
		O(3)¹ — Th — O(3)⁶	142.0(2)
		O(3)¹ — Th — O(3)⁵	119.1(2)

(b) Calcium coordination, distorted tetrahedron.

Ca — O(3) 2.342(5)Å

Non-bonded contacts, (Å).		Angles(°)	
O(3)¹... O(3)⁸ 2.920(6)		O(3)¹ — Ca — O(3)⁸	139.8(2)
O(3)¹... O(3)⁹ 4.000(7)		O(3)¹ — Ca — O(3)⁹	117.3(2)
O(3)¹... O(3)¹⁰ 4.398(7)		O(3)¹ — Ca — O(3)¹⁰	77.1(2)

(c) Silicate tetrahedron.

Si — O(1) — Si 147.8(4)°

For other bond lengths and angles, see Fig. 5.

Non-bonded contacts, (Å).		
O(1) ... O(2) 2.624(5)		O(1) ... O(1)¹² 2.649(7)
O(1) ... O(3) 2.658(6)		O(2) ... O(1)¹² 2.690(7)
O(2) ... O(3) 2.629(5)		O(3) ... O(1)¹² 2.533(7)

Superscripts used above and in the diagrams refer to the following equivalent positions:-

1.	x , y , z	7.	y , $-x$, z
2.	y , x , $-z$	8.	x , $-y$, $-z$
3.	y , $-x$, z	9.	$1-x$, $-y$, z
4.	$-x$, y , $-z$	10.	$1-x$, y , $-z$
5.	$-x$, $-y$, z	11.	$1-y$, $-x$, $-z$
6.	$-y$, $-x$, $-z$	12.	$1-y$, x , z

$x,\frac{1}{2},0.3$; $x,\frac{1}{2},0.7$; $0,y,0.2$; $0,y,0.8$; $\frac{1}{2},y,0.3$; $\frac{1}{2},y,0.7$. The "walls" of these channels consist of all three types of oxygens in the structure: O(1), O(2) and O(3).

DISCUSSION

The channels mentioned above provide the explanation for the non-structural water content of the mineral. These channels are large enough to provide easy passage for any water molecules in a zeolite-like fashion. Furthermore, as the "walls" are composed of oxygens, this water can easily form a hydrogen-bonded network within the structure. It need not be structurally repetitive and regular, and will thus not affect the diffracted intensities significantly other than the contribution to thermal diffuse scattering and to the background.

When heated at 900°C for three hours, a specimen of the mineral lost weight from 65 to 59 mg with no change in the powder pattern. This corresponds to a composition of about 9.5 water molecules per unit cell. Certainly, there is room in the structure to accommodate more than this, and it may be that the water molecules within the cell are mobile.

The only significant nonstoichiometry occurs at the thorium site, which has a site occupancy of about 94%; within this remainder, about 5% uranium substitutes for thorium. The thorium is contained within a square antiprism of O(3) oxygens, and the sides of the square are about 4.15 Å.

Radioactive decay of both thorium and uranium yields isotopes of radon which, not being coordinated to water, could easily escape through the O(3) square and into the infinite channels. Being both a gas and also water soluble, radon could easily escape from the structure through either gaseous emanation or water leaching, prior to its decay to lead. No lead was found in the analyses. However, it is impossible to say with any certainty whether the mineral actually crystallized with some deficiency in the thorium

site, or whether the incomplete site-occupancy at this site is the result of radioactive decay.

COMPARISON WITH THE STRUCTURE OF STEACYITE

The structure of steacyite (Richard & Perrault 1972) has been redrawn in Figure 4 to extend from $z = \frac{1}{4}$ to $1\frac{1}{4}$. The segment of the structure of ekanite from $z = 0$ to $z = \frac{1}{4}$ is virtually identical with the segment of the structure of steacyite from $z = \frac{1}{4}$ to $z = \frac{1}{2}$. This can be seen readily from a comparison of

the x co-ordinates given beside each atom. The principal difference between these slices of the two structures is that steacyite contains potassium at $0,0,\frac{1}{2}$, whereas in ekanite the corresponding site, $0,0,\frac{1}{4}$, is vacant. The square antiprism co-ordination of Th, the distorted tetrahedral co-ordination of the nearest neighbors, and the second-nearest neihbors around Ca are very similar. There are differences in the bond lengths in the two minerals: Th–O(3) = 2.405(5), 2.413(5), Ca–O(3) = 2.342(5), 2.447(5), Ca–O(second-nearest neighbors) = 2.688(5), 2.631(5) Å for ekanite and steacyite,
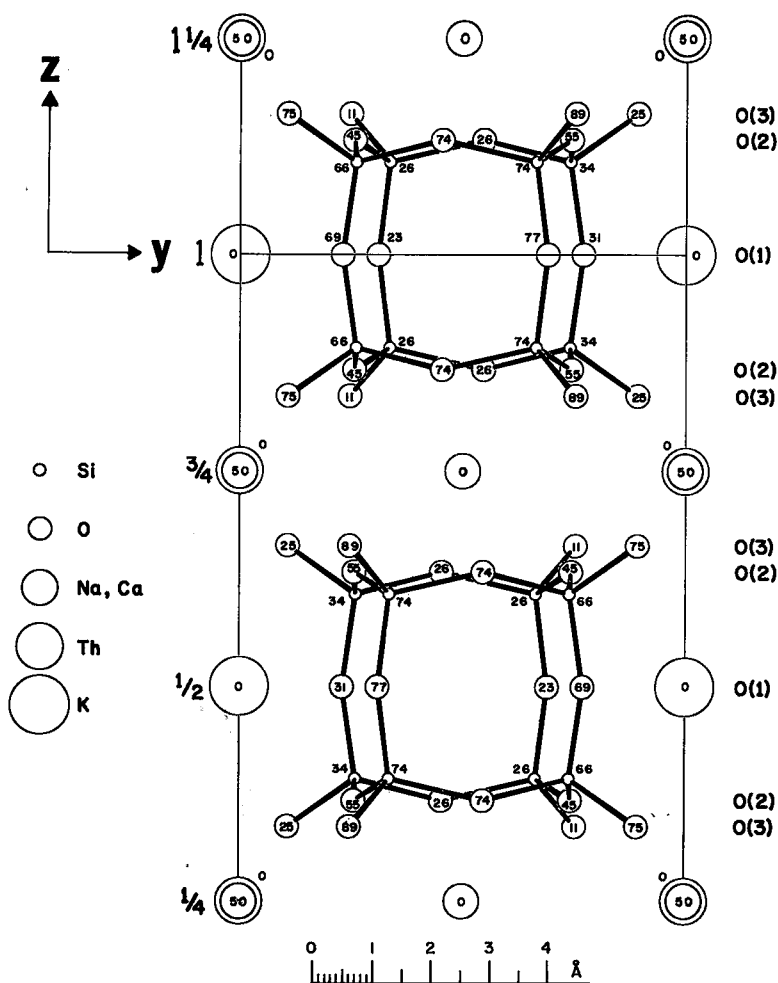

FIG. 4. The crystal structure of steacyite (Richard & Perrault 1972) projected on the y–z plane from $z = \frac{1}{4}$ to $1\frac{1}{4}$. Other than the presence of K at $0,0,\frac{1}{2}$, the slice of the unit cell from $z = \frac{1}{4}$ to $z = \frac{1}{2}$ can be nearly superimposed on the corresponding slice ($z = 0$ to $\frac{1}{4}$) of the ekanite structure.

respectively. The square antiprism of co-ordinating oxygens around Th is somewhat more
regular in ekanite than in steacyite. The triangle of three oxygens that make up the side face
of the antiprism has sides 2.932(7), 2.896(6),
2.902(6) Å, and angles 60.6(2), 59.3(2) and
60.1(2)° in ekanite. The corresponding values
in steacyite are 2.891(7), 2.966(7), 3.043(7) Å
and 57.5(2), 59.9(2) and 62.6(2)°.

The principal difference in the structures of
the two minerals is found in the silicate network. In ekanite, the first square of silicate
tetrahedra is virtually identical to that found
in steacyite, but in the latter structure, a centre
of symmetry at (½,½,½) gives rise to a second
square above the first. The tetrahedra of the
two squares share corners [O(1)] to form discrete Si_8O_{20} cubes (Fig. 4). As already explained, in ekanite, oxygens O(2) connect
squares of tetrahedra within the same sheet,
but at two different levels in z. These squares
are formed around different four-fold axes.
There are, therefore, no discrete silicon–oxygen
units in ekanite, but rather infinite sheets in the
x–y plane.

The geometry of the silicate group in ekanite,
shown in Figure 5, is very similar to that found
in steacyite. In the present structure ·there are
two longer Si–O bonds [1.640(5), 1.632(5)
Å], and these are to the oxygens that are involved in the corner-sharing to form Si–O–Si–
O– links within a given square of tetrahedra.
In steacyite, these bonds are also longer [1.639

(5), 1.625(5) Å]. The Si–O bonds of O(3)
(the Th and Ca co-ordinating oxygen) and of
O(2) (the oxygen that links squares of tetrahedra) are virtually identical in ekanite [1.584
(5), 1.589(2) Å] but are somewhat different
in steacyite [1.572(5), 1.601(3) Å]. There are
significant differences between the two structures in the angular distortions of the silicate
tetrahedra, but this is not unexpected in view
of the two different ways in which the squares
of tetrahedra are linked.

Steacyite also contains channels through the
silicate network where nonstructural water can
be entrapped (3–14% by weight: Perrault &
Richard 1973). However, ekanite has twice as
many channels as steacyite, because in the latter
structure, half the corresponding channels are
blocked by potassium ions. This makes ekanite
even more porous than steacyite on an atomic
scale.

REFERENCES

ANDERSON, B.W., CLARINGBULL, G.F., DAVIS, R.J.
& HILL, D.K. (1961): Ekanite, a new metamict
mineral from Ceylon. *Nature* 190, 997.

BOND, W.L. (1951): Making small spheres. *Rev.
Sci. Instr.* 22, 344-345.

BUSING, W.R. (1970): Least-squares refinement of
lattice and orientation parameters for use in
automatic diffractometry. *In* Crystallographic
Computing (F.R. Ahmed, ed.). Munksgaard,
Copenhagen.

EMBREY, P.G. & FULLER, J.P., eds. (1980): *A
Manual of New Mineral Names*. Oxford University Press, Oxford, England.

FARRELL, D.M. (1978): Infrared investigation of
an unidentified hydroxo calcium thorium silicate
from the Yukon Territory. *CANMET Rep.
MRP/MSL* 78–115(TR). Dep. Energy, Mines,
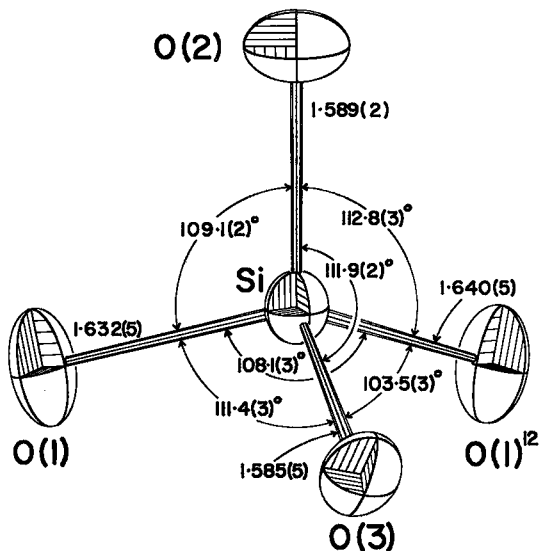Res., Ottawa, Ont.

FIG. 5. The SiO_4 group viewed parallel to the [110]
direction, showing bond lengths and angles.

GINZBURG, I.V., SEMENOV, E.J., LEONOVA, L.L., SIDORENKO, G.A. & DUSMATOV, V.D. (1965): Alkali-rich crystalline ekanite from central Asia. *In* New Data on Minerals of the U.S.S.R. Academy of Sciences of the U.S.S.R., Moscow (in Russ.).

GÜBELIN, E.J. (1961): Ekanite. *Gems Gemmology* 10, 165-179.

———— (1962): Ekanite. *Gemmologist* 31, 142-159, 165-169.

HALL, S.R. & SZYMAŃSKI, J.T. (1975): Powder pattern generation from single-crystal data. *Amer. Cryst. Assoc. Winter Meet., Abstr.* F13. Now incorporated in the XRAY–76 system of programs [see Stewart *et al.* (1976)].

HEY, M.H. & EMBREY, P.G. (1974): Twenty-eighth list of new mineral names. *Mineral. Mag.* 39, 903-932.

IBERS, J.A. & HAMILTON, W.C., eds. (1974): *International Tables for X-ray Crystallography. IV. Revised and Supplementary Tables.* Int. Union Cryst., the Kynoch Press, Birmingham, England.

JOHNSON, C.K. (1965): ORTEP: A FORTRAN thermal ellipsoid plot program for crystal structure illustrations. *Rep.* ORNL-3794, 2nd Rev. ORTEP-II addition 1971, *Oak Ridge Nat. Lab.*, Oak Ridge, Tennessee; modified for use in the X-RAY STEWART System by J.F. Guédon, S. Hall, P. Richard and S. Whitlow.

LIVINGSTONE, A., ATKIN, D., HUTCHINSON, D. & AL-HERMEZI, H.M. (1976): Iraqite, a new rare-earth mineral of the ekanite group. *Mineral. Mag.* 40, 441-445.

MOKEYEVA, V.I. & GOLOVASTIKOV, N.I. (1966): The crystal structure of ekanite $ThK[Ca,Na]_2Si_8O_{20}$. *Dokl. Akad. Nauk S.S.S.R.* 167, 1131-1134 (in Russ.; translation in *Dokl. Acad. Sci. U.S.S.R., Earth Sci. Sect.* 167, 106-108).

OKAYA, Y., SAITO, Y. & PEPINSKY, R. (1955): New method in X-ray crystal structure determination involving the use of anomalous dispersion. *Phys. Rev.* 98, 1857-1858.

PERRAULT, G. & RICHARD, P. (1973): L'ekanite de Saint-Hilaire, P.Q. *Can. Mineral.* 11, 913-929.

———— & SZYMAŃSKI, J.T. (1982): Steacyite, a new name, and a re-evaluation of the nomenclature of "ekanite" — group minerals. *Can. Mineral.* 20, 59-63.

POVARENNYKH, A.S. & DUSMATOV, V.D. (1970): Infrared absorption spectra of new minerals from alkaline pegmatites of central Asia. *Konst. Svoistva Mineralov, Akad. Nauk Ukr. S.S.R., Respub. Mezhvedom. Sb.* 4, 3-9.

RICHARD, P. & PERRAULT, G. (1972): La structure cristalline de l'ekanite $Th_{2-x}(Na,Ca)_{4-y}K_{2-z}Si_{16}O_{40}$. *Acta Cryst.* B28, 1994-1999.

STEWART, J.M., MACHIN, P.A. DICKINSON, C.W., AMMON, H.L., HECK, H. & FLACK, H. (1976): The X–RAY system of crystallographic programs. *Univ. Maryland Comp. Sci. Ctr. Tech. Rep.* TR–446.